Prediction Model (CCIR-1978a, Doc. P/105-E, 6 June), employs a path averaging parameter "r" to relate the point rain rate to the average rain rate along the path from the ground station to the point where the hydrometeors exist in the form of ice crystals. The later form of the model (Crane and Blood - 1979, Crane - 1980a, 1980b) includes path averaging implicitly, and adjusts the isotherm heights for various percentages of time to account for the types of rain structures which dominate the cumulative statistics for the respective percentages of time. Both forms will be described here because the latter is the recommended form for use by system designers, but the earlier form is computationally easy to implement and allows rapid computation with a hand-held calculator.

3.4.1 Rain Model

The rain model employed in both forms of the attenuation model is used for the estimation of the annual attenuation distribution to be expected on a specific propagation link. It differs from most other rain models in that it is based entirely on meterological observations, not attenuation measurements. The rain model, combined with the attenuation estimation, was tested by comparison with attenuation measurements. This procedure was used to circumvent the requirement for attenuation observations over a span of many years. The total attenuation model is based upon the use of independent, meteorologically derived estimates for the cumulative distributions of point rainfall rate, horizontal path averaged rainfall rate, the vertical distribution of rain intensity, and a theoretically derived relationship between specific attenuation and rain rate obtained using median observed drop size distributions at a number of rain rates.

The first step in application of the model is the estimation of the instantaneous point rain rate (R_p) distribution. The Global Prediction Model provides median distribution estimates for broad geographical regions; eight climate regions A through H are designated to classify regions covering the entire globe.

Figures 3.4-1 and 3.4-2 show the geographic rain climate regions for the continental and ocean areas of the earth. The United States and European portions are further expanded in Figures 3.4-3 and 3.4-4 respectively.

The climate regions depicted by the Global Model are very broad. The upper and lower rain rate bounds provided by the nearest adjacent region have a ratio of 3.5 at 0.01 percent of the year for the proposed CCIR climate region D, for example, producing an attendant ratio of upper-to-lower bound attenuation values of 4.3 dB at 12 GHz. This uncertainty in the estimated attenuation value can be reduced by using rain rate distributions tailored to a particular area if long term statistics are available. Using the subdivision of climate regions B and D in the continental United States, Canada, and Europe also helps to reduce the uncertainty in the estimates.

The values of R_p may be obtained from the rain rate distribution curves of Figure 3.4-5. Figure 3.4-5a shows the curves for the eight global climate regions designated A through H for one minute averaged surface rain rate as a function the percent of year that rain rate is exceeded. The distributions for the region B and D subregions are shown in Figure 3.4-5b. Note that the distribution for region D_2 corresponds to that for D. Numerical values of R_p are provided in Table 3.4-1 for all regions and subregions.

3.4.2 Description of the Rain Attenuation Region

A path averaged rainfall rate $R = rR_p$, where r is defined as the effective path average factor, is useful for the estimation of attenuation for a line-of-sight radio relay system but, for the estimation of attenuation on a slant path to a satellite, account must be taken of the variation of specific attenuation with height. The atmospheric temperature decreases with height and, above some height, the precipitation particles must all be ice particles. Ice or snow do not produce significant attenuation; only regions with liquid water precipitation particles are of interest in the

Table 3.4-1. Point Rain Rate Distribution Values (mm/hr) Versus Percent of Year Rain Rate is Exceeded

Percent of Year	RAIN CLIMATE REGION												Minutes per Year	Hours per Year
	A	B_1	B	B_2	C	D_1	$D=D_2$	D_3	E	F	G	H		
0.001	28.5	45	57.5	70	78	90	108	126	165	66	185	253	5.26	0.09
0.002	21	34	44	54	62	72	89	106	144	51	157	220.5	10.5	0.18
0.005	13.5	22	28.5	35	41	50	64.5	80.5	118	34	120.5	178	26.3	0.44
0.01	10.0	15.5	19.5	23.5	28	35.5	49	63	98	23	94	147	52.6	0.88
0.02	7.0	11.0	13.5	16	18	24	35	48	78	15	72	119	105	1.75
0.05	4.0	6.4	8.0	9.5	11	14.5	22	32	52	8.3	47	86.5	263	4.38
0.1	2.5	4.2	5.2	6.1	7.2	9.8	14.5	22	35	5.2	32	64	526	8.77
0.2	1.5	2.8	3.4	4.0	4.8	6.4	9.5	14.5	21	3.1	21.8	43.5	1052	17.5
0.5	0.7	1.5	1.9	2.3	2.7	3.6	5.2	7.8	10.6	1.4	12.2	22.5	2630	43.8
1.0	0.4	1.0	1.3	1.5	1.8	2.2	3.0	4.7	6.0	0.7	8.0	12.0	5260	87.7
2.0	0.1	0.5	0.7	0.8	1.1	1.2	1.5	1.9	2.9	0.2	5.0	5.2	10520	175
5.0	0.0	0.2	0.3	0.3	0.5	0.0	0.0	0.0	0.5	0.0	1.8	1.2	26298	438

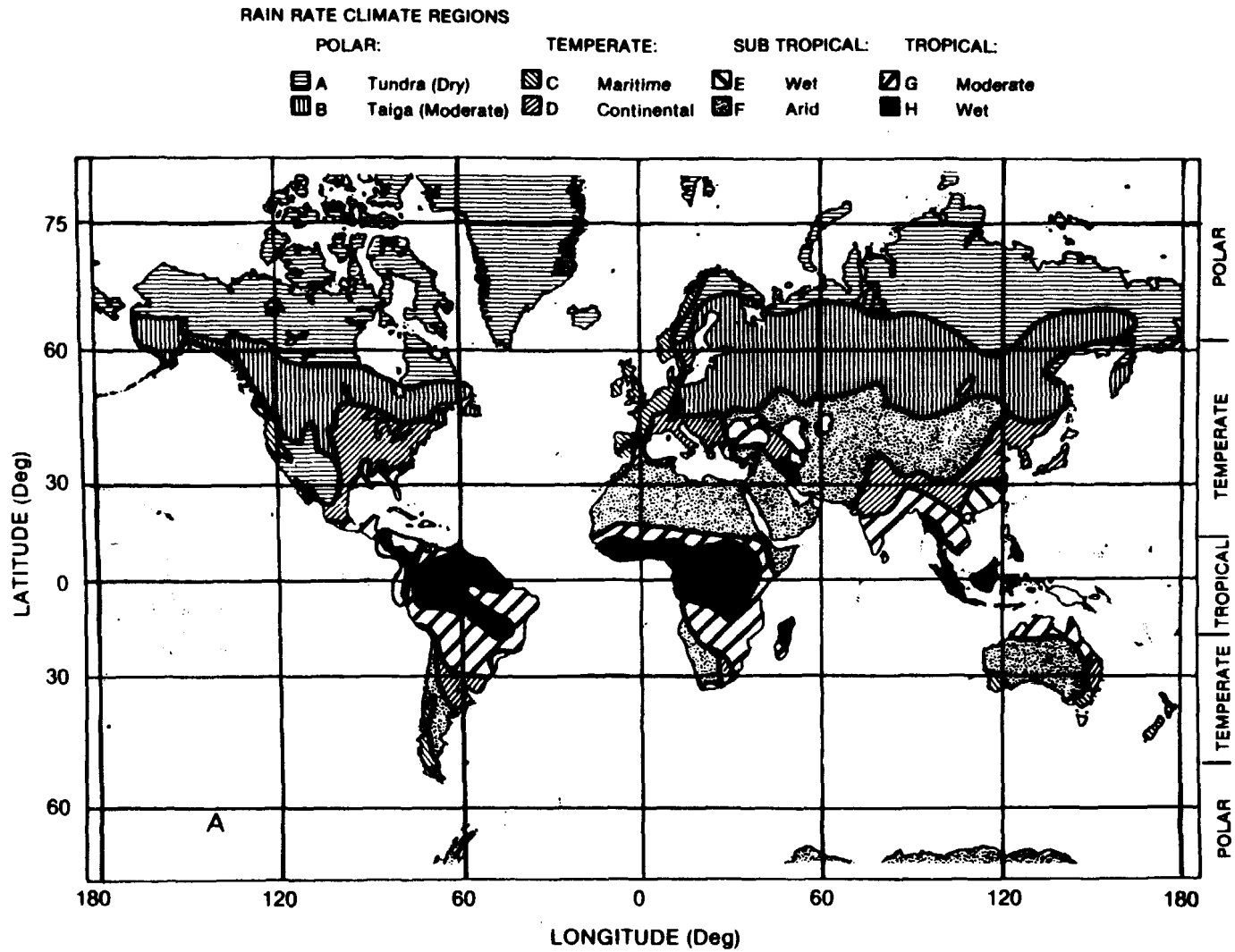

Figure 3.4-1. Global Rain Rate Climate Regions for the Continental Areas

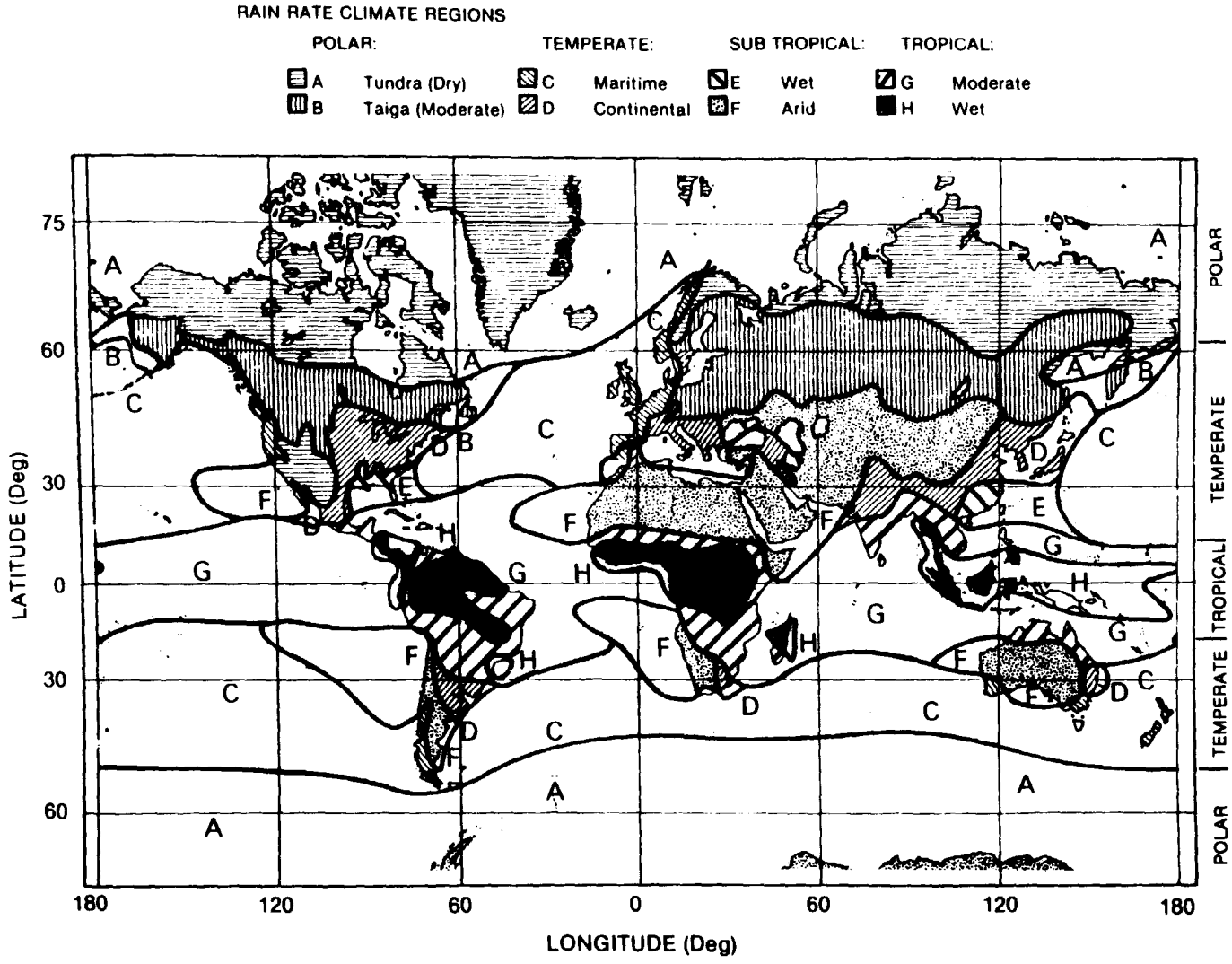

Figure 3.4-2. Global Rain Rate Climate Regions Including the Ocean Areas

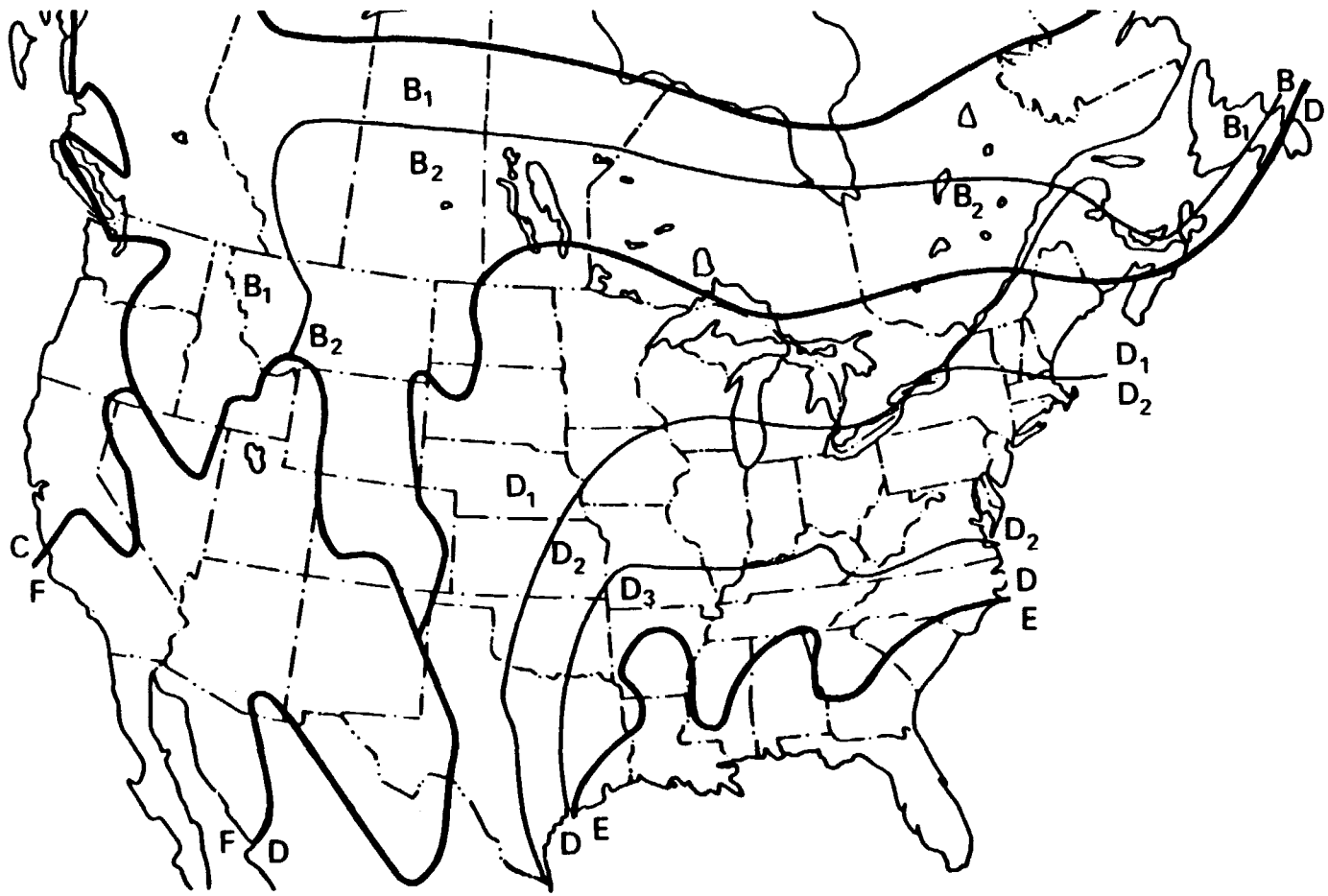

Figure 3.4-3. Rain Rate Climate Regions for the Continental U.S. and Southern Canada

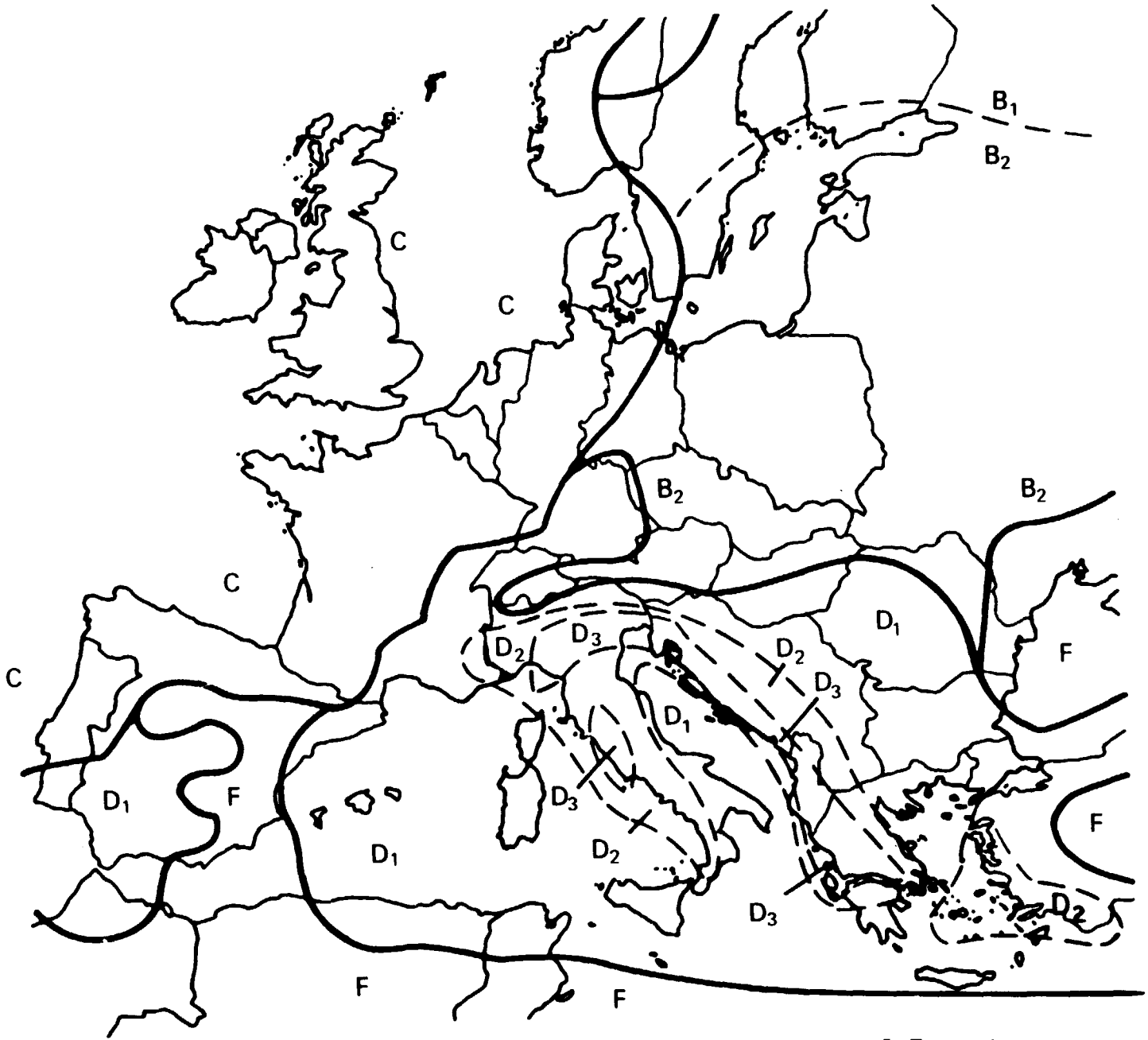

Figure 3.4-4. Rain Rate Climate Regions of Europe

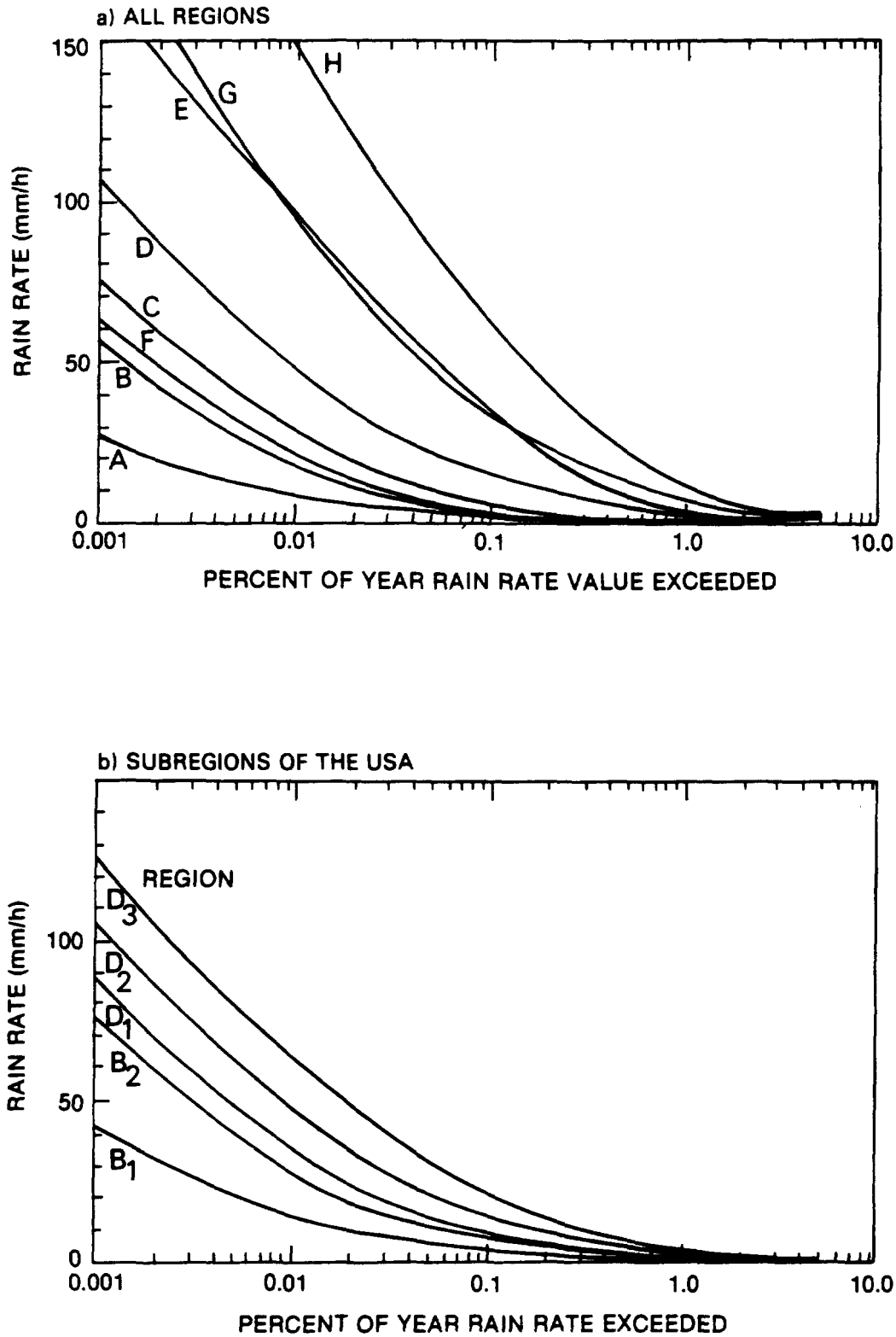

Figure 3.4-5. Point Rain Rate Distributions as a Function of Percent of Year Exceeded

estimation of attenuation. The size and number of rain drops per unit volume may vary with height. Measurements made using weather radars show that the reflectivity of a rain volume may vary with height but, on average, the reflectivity is roughly constant with height to the height of the 0°C isotherm and decreases above that height. The rain rate may be assumed to be constant to the height of the 0°C isotherm at low rates and this height may be used to define the upper boundary of the attenuating region. A high correlation between the 0°C height and the height to which liquid rain drops exist in the atmosphere should not be expected for the higher rain rates because large liquid water droplets are carried aloft above the 0° height in the strong updraft cores of intense rain cells. It is necessary to estimate the rain layer height appropriate to the path in question before proceeding to the total attenuation computation since even the 0°C isotherm height depends on latitude and general rain conditions.

As a model for the prediction of attenuation, the average height of the 0° isotherm for days with rain was taken to correspond to the height to be expected one percent of the year. The highest height observed with rain was taken to correspond to the value to be expected 0.001 percent of the year, the average summer height of the -5°C isotherm. The latitude dependences of the heights to be expected for surface point rain rates exceeded one percent of the year and 0.001 percent of the year were obtained from the latitude dependences provided by Oort and Rasmussen (1971). The resultant curves are presented in Figure 3.4-6. For the estimation of model uncertainty, the seasonal rms uncertainty in the 0°C isotherm height was 500 m or roughly 13 percent of the average estimated height. The value of 13 percent is used to estimate the expected uncertainties to be associated with Figure 3.4-6.

The correspondence between the 0°C isotherm height values and the excessive precipitation events showed a tendency toward a linear relationship between R_p and the 0°C isotherm height H_o for high values of R_p. Since, at high rain rates, the rain rate distribution

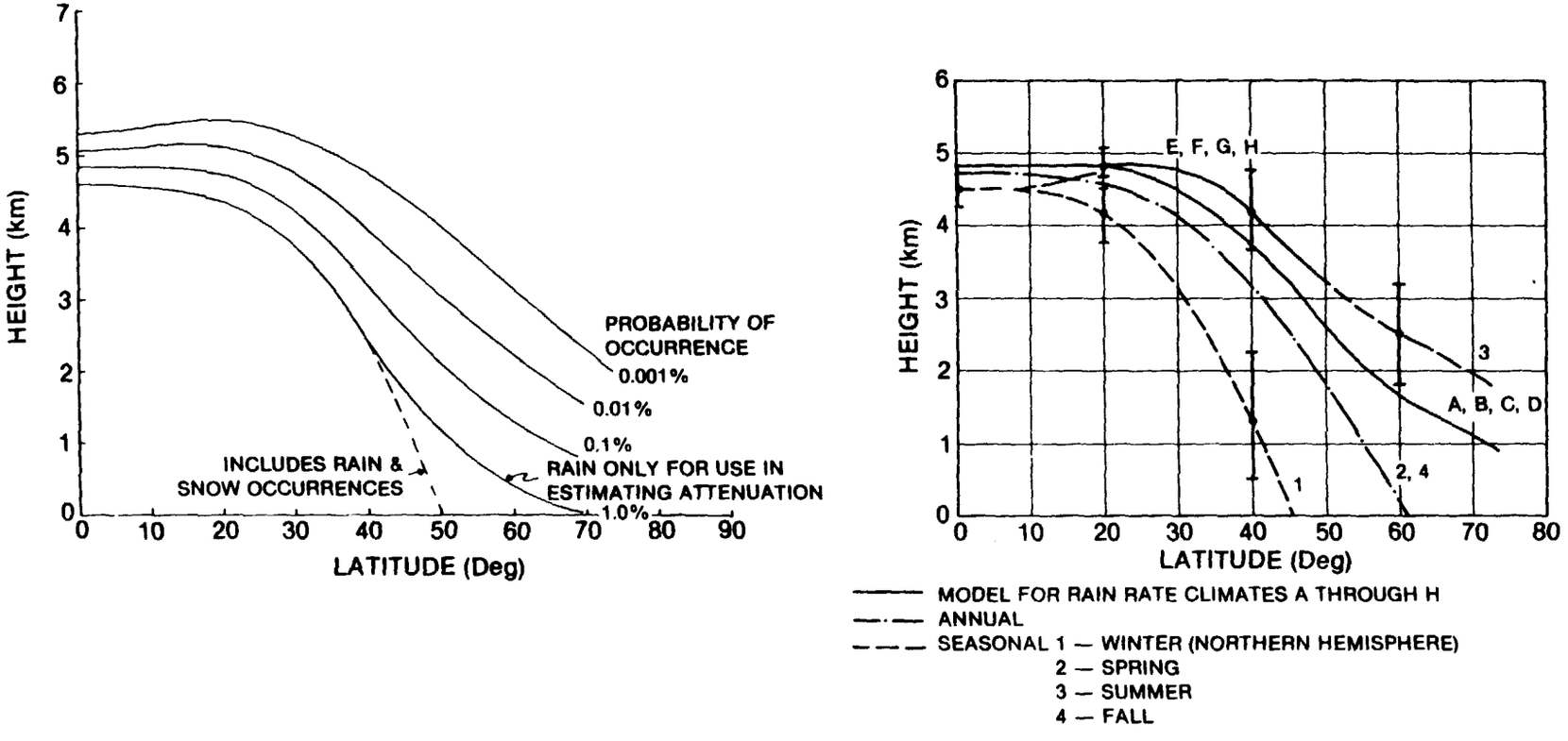

a) Variable Isotherm

b) $0^{o}C$ Isotherm Height

Figure 3.4-6. Effective Heights for Computing Path Lengths Through Rain Events

function displays a nearly linear relationship between R_p and log P (P is probability of occurrence), the interpolation model used for the estimation of H_o for P between 0.001 and one percent is assumed to have the form, $H_o = \underline{a} + \underline{b} \log P$. The relationship was used to provide the intermediate values displayed in Figure 3.4-6a. In Figure 3.4-6b are shown the 0°C isotherms for various latitudes and seasons.

3.4.3 Attenuation Model

The complete model for the estimation of attenuation on an earth-space path starts with the determination of the vertical distance between the height of the earth station and the 0°C isotherm height ($H_0 - H_g$ where H_g is the ground station height) for the percentage of the year (or R_p) of interest. The path horizontal projection distance (D) can then be obtained by:

$$D = \begin{cases} (H_o - H_g)/\tan\theta & \theta \geq 10^\circ \\ E\psi \ (\psi \text{ in radians}) & \theta < 10^\circ \end{cases} \qquad (3.4\text{-}1)$$

where

H_o = height of 0°C isotherm

H_g = height of ground terminal

θ = path elevation angle

and

$$\psi = \sin^{-1}\left\{\frac{\cos\theta}{H_o + E}\left[(H_g + E)^2 \sin^2\theta + 2E(H_o - H_g) + H_o^2 - H_g^2\right]^{1/2} - (H_g + E)\sin\theta\right\} \qquad (3.4\text{-}2)$$

$$= \cos^{-1}\left[\frac{\cos\theta}{H_o + E}(E + H_g)\right] - \theta$$

where

E = effective earth's radius (8500 km).

The specific attenuation may be calculated for an ensemble of rain drops if their size and shape number densities are known. Experience has shown that adequate results may be obtained if the Laws and Parsons (1943) number density model is used for the attenuation calculations (Crane-1966) and a power law relationship is fit to calculated values to express the dependence of specific attenuation on rain rate (Olsen et al-1978). The parameters a and b of the power law relationship:

$$\alpha = aR_p^b \qquad (3.4\text{-}3)$$

where α = specific attenuation (dB/km)

R_p = point rain rate (mm/hour)

are both a function of operating frequency. Figures 3.4-7 and 3.4-8 give the -multiplier, a(f) and exponent b(f), respectively, at frequencies from 1 to 100 GHz. The appropriate a and b parameters may also be obtained from Table 3.4-2 and used in computing the total attenuation from the model. Alternately, values of a and b from Tables 2.3-2 or 2.3-3 may be used.

3.4.3.1 Path Averaged Rain Rate Technique. The path averaged rain rate exceeded for a specified percentage of the time may differ significantly from the surface point rain rate exceeded for the same percentage of the time. The estimation of the path averaged values from the surface point values requires detailed information about the spatial correlation function for rain rate. Adequate spatial data are not currently available. A sufficient number of observations using rain guage networks are available to provide a basis for a point to path average model. Observations for 5 and 10 km paths are presented in Figures 3.4-9 and 3.4-10, respectively. The effective path average factor, r, represents the relationship between point and path averaged rain rate as

$$R_{path} = r \cdot R_p \qquad (3.4\text{-}4)$$

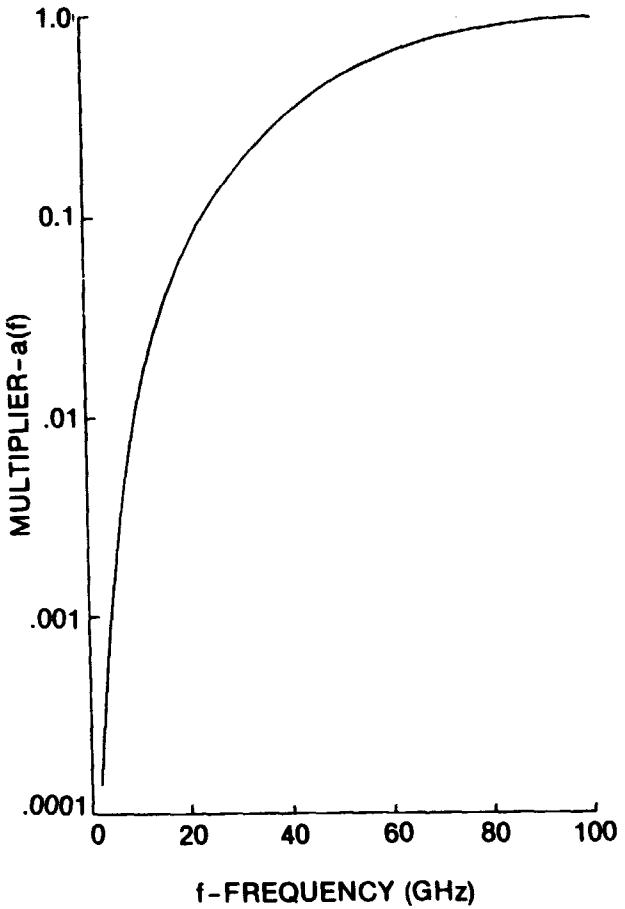

Figure 3.4-7. Multiplier Coefficient in the Specific Attenuation Relation

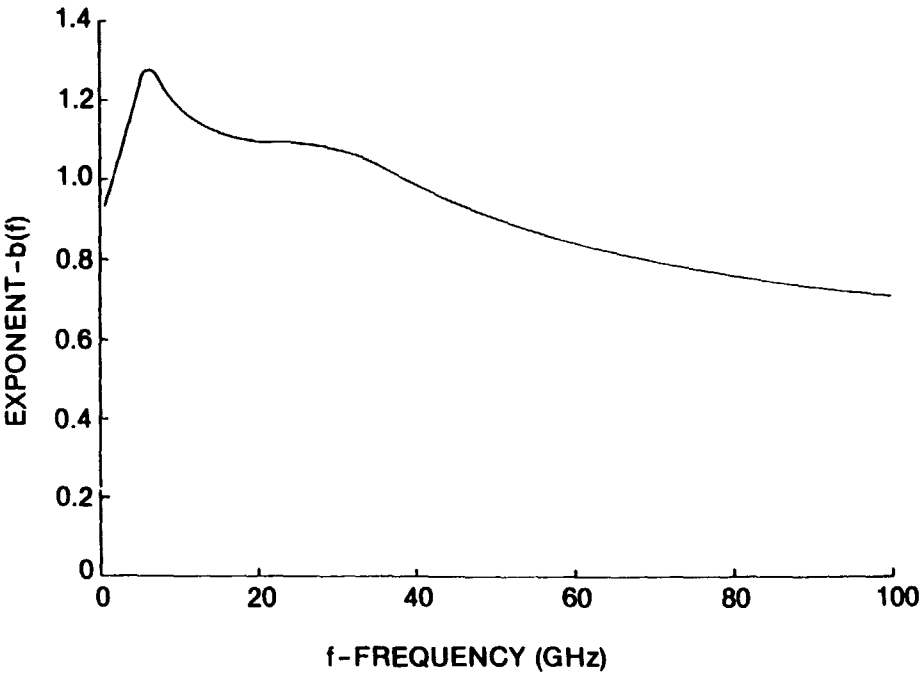

Figure 3.4-8. Exponent Coefficient in the Specific Attenuation Relation

Table 3.4-2. Parameters for Computing Specific Attenuation: $= aR^b$, 0°C, Laws and Parson Distribution (Crane-1966)

Frequency f - GHz	Multiplier a(f)	Exponent b(f)
1	0.00015	0.95
4	0.00080	1.17
5	0.00138	1.24
6	0.00250	1.28
7.5	0.00482	1.25
10	0.0125	1.18
12.5	0.0228	1.145
15	0.0357	1.12
17.5	0.0524	1.105
20	0.0699	1.10
25	0.113	1.09
30	0.170	1.075
35	0.242	1.04
40	0.325	0.99
50	0.485	0.90
60	0.650	0.84
70	0.780	0.79
80	0.875	0.753
90	0.935	0.730
100	0.965	0.715

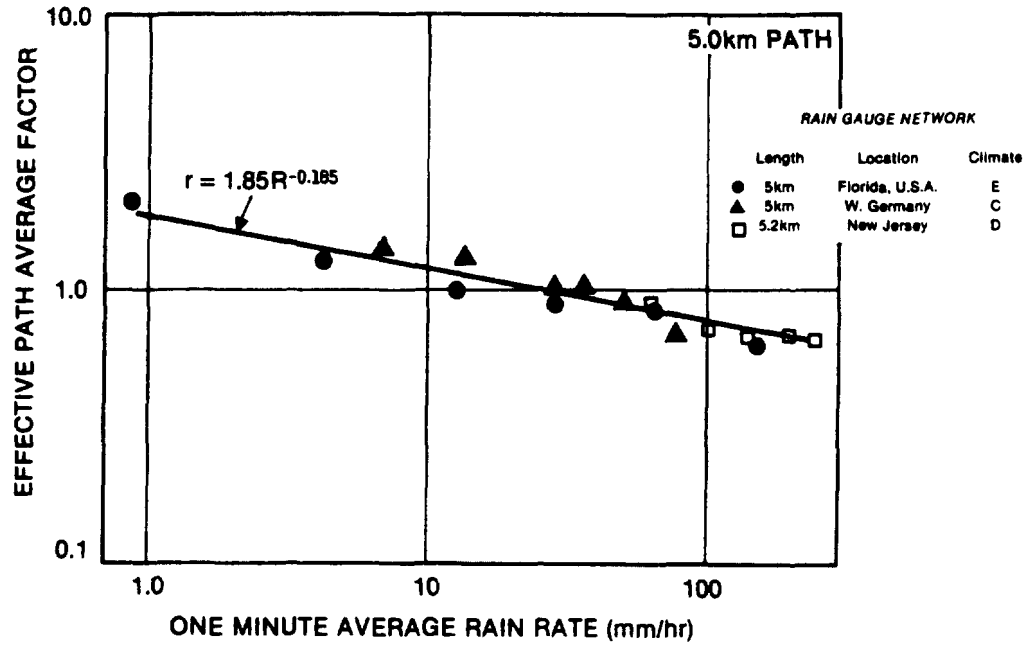

Figure 3.4-9. Effective Path Average Factor Versus Rain Rate, 5 km Path

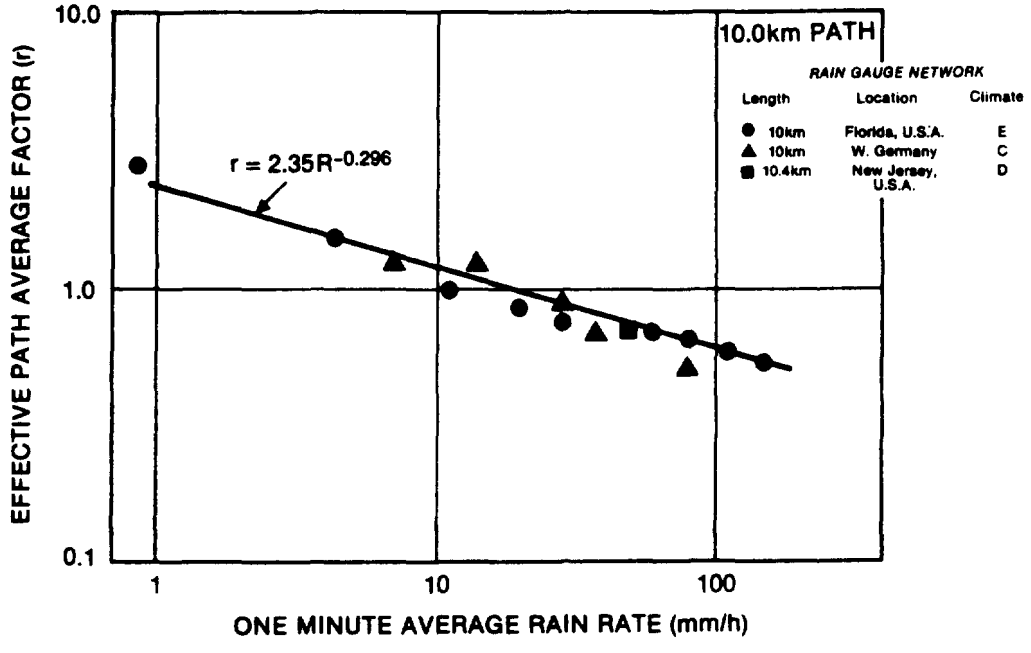

Figure 3.4-10. Effective Path Average Factor Versus Rain Rate, 10 km Path

where R_{path} and R_p are the path and point rainfall rates at the same probability of occurrence.

Figure 3.4-11 represents the construction of an effective path average factor using data from paths between 10 and 22.5 km in length. The values of r were obtained by assuming that the occurrence of rain with rates in excess of 25 mm/hour were independent over distances larger than 10 km. The estimation of path averaged rain rate then depends upon modeling the change in occurrence probability for a fixed path average value, not the change in path average value for a fixed probability. Using D_o as the reference path length (D_o = 22.5 km for Figure 3.4-11), the exceedance probabilities for the path averaged values were multiplied by D_o/D where D was the observation path length to estimate the path average factor for a path of length D_o.

The path attenuation caused by rain is approximately determined from the path averaged rain rate by

$$A \approx L\ r\ a\ R_p^b \qquad (3.4\text{-}5)$$

where A is path attenuation, L is the length of the propagation path or D_o, whichever is shorter, r is the effective path average factor, R is the point rainfall rate exceeded P percent of the time, and a and b are coefficients used to estimate specific attenuation for a given rain rate. Using this model and propagation paths longer than 22.5 km, the effective path average factor for 22.5 km path may be calculated from simultaneous point rain rate distribution and attenuation distribution data. Results for a number of paths in rain rate climates C and D are presented in Figure 3.4-12. The line plotted on this figure is the power law relationship fit to all the data displayed in Figure 3.4-11. The observations at 13 and 15 GHz are in excellent agreement with the model based solely on rain gauge network data. At lower frequencies, the discrepancy is larger, being as much as a factor of 2. At 11 GHz, the model appears to underestimate the observed attenuation by a factor of 2. It is

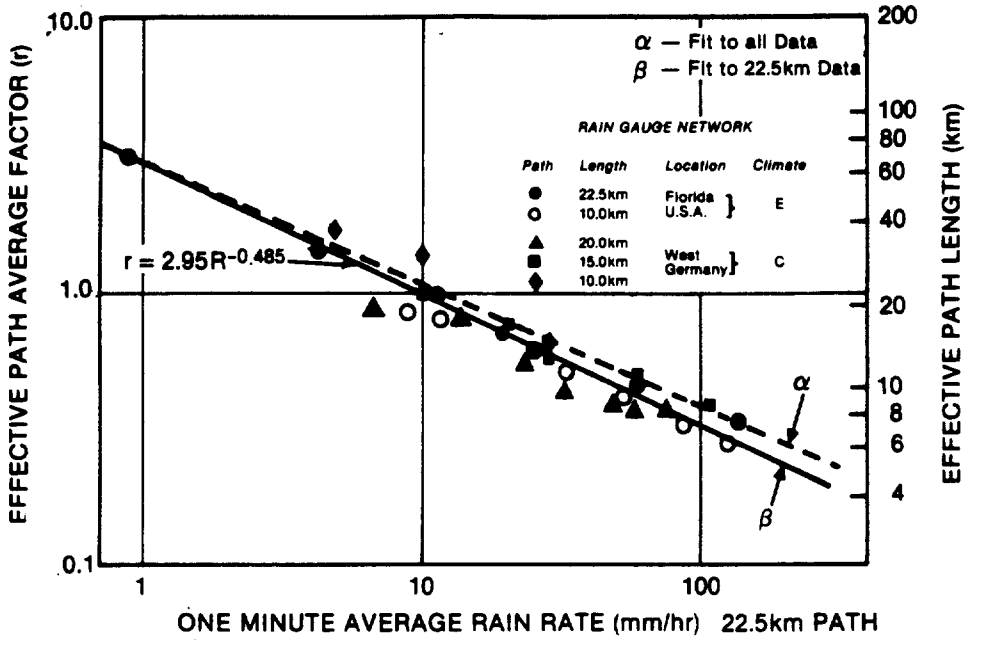

Figure 3.4-11. Effective Path Average Factor Versus Rain Rate

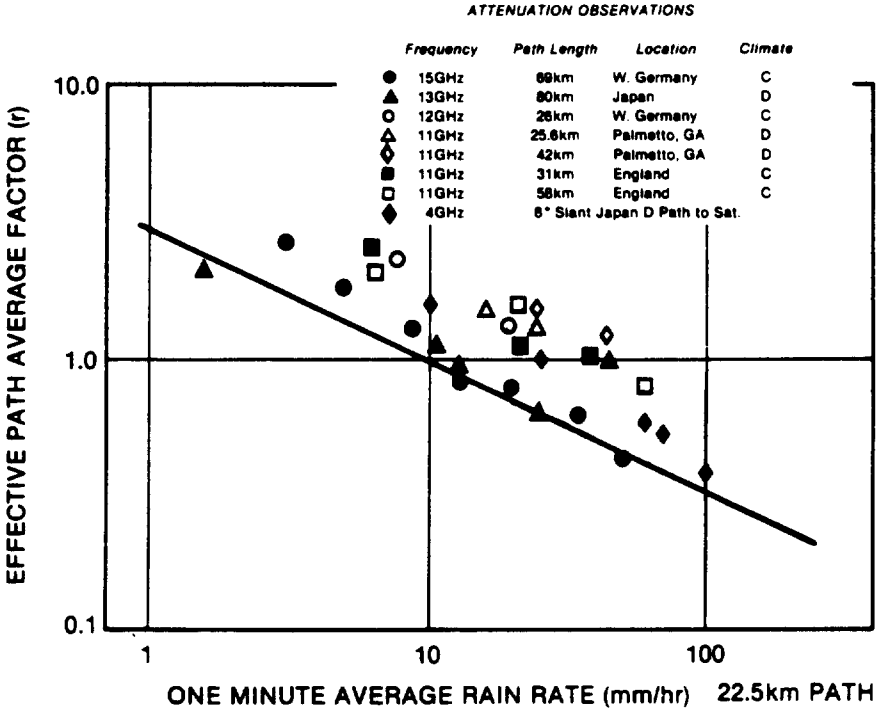

Figure 3.4-12. Effective Path Average Factor Versus Rain Rate Derived from Attenuation Measurements

noted that simultaneous point rain rate observations were used in the construction of Figure 3.4-12, not the rain rate distributions for each climate region. Since fades due to multipath must be removed from the analysis prior to making the comparison in Figure 3.4-12 and multipath effects tend to be relatively more important at frequencies below 13 GHz, the lack of agreement displayed in Figure 3.4-12 may be due to effects other than rain.

A power law approximation to the effective path average factors depicted in Figures 3.4-9 through 3.4-11 may be used to model the behavior of the effective path average factor for paths shorter than 22.5 km. Letting the effective path average factors be expressed by

$$r \approx \gamma(D) R_p^{-\delta(D)} \qquad (3.4\text{-}6)$$

where D is the surface projection of the propagation path and the model curves for $\gamma(D)$ and $\delta(D)$ are given in Figure 3.4-13 and 3.4-14. Figure 3.4-15 displays the dependence of the modeled effective path average factor on point rain rate.

Attenuation prediction for Earth-space paths requires the estimation of rain rate along a slant path. Statistical models for rain scatter indicate that the reflectivity, hence, specific attenuation or rain rate, is constant from the surface to the height of the OoC isotherm (Goldhirsh and Katz 1979). By assuming that the specific attenuation is statistically independent of height for altitudes below the O°C isotherm the path averaged rain rate (or specific attenuation) can be estimated using the model in Figures 3.4-13 and 3.4-14. For application, the surface projection of the slant path below the melting layer is used to define the surface path length, D. The attenuation on an Earth-space path for an elevation angle higher than 10° is given by:

$$A = \frac{H}{\sin\theta}\, a(f)\, \gamma(D)\, R_p^{b(f)-\delta(D)} \qquad (3.4\text{-}7)$$

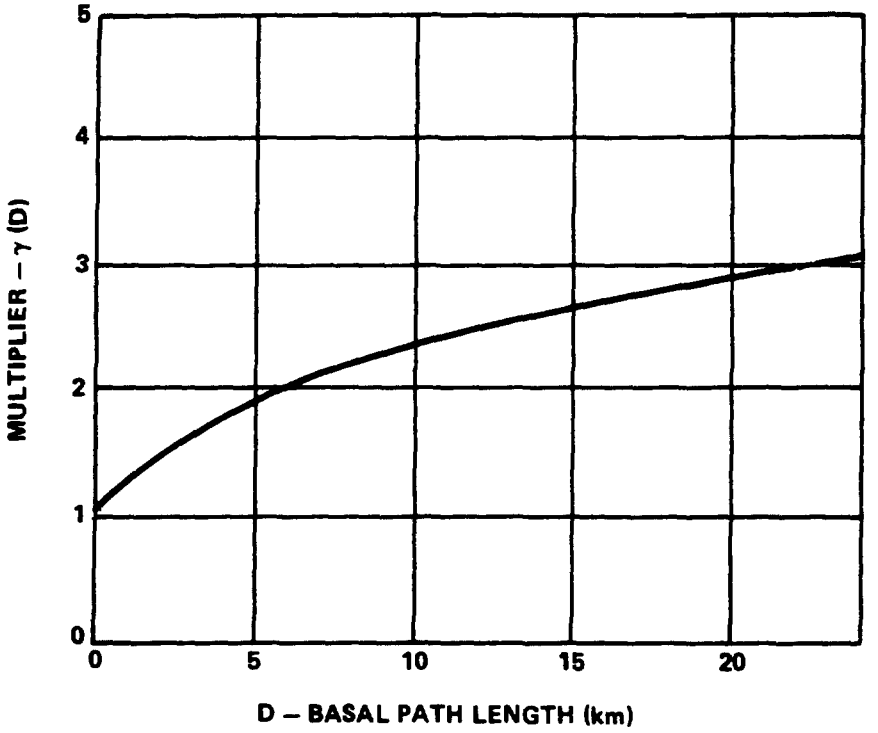

Figure 3.4-13. Multiplier in the Path Averaging Model

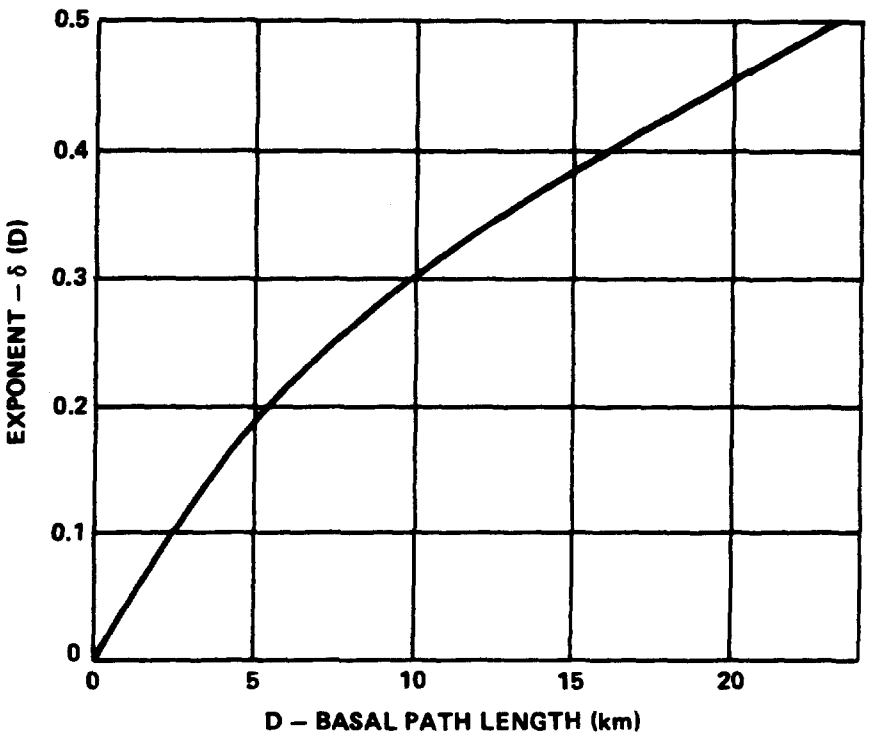

Figure 3.4-14. Exponent in the Path Averaging Model

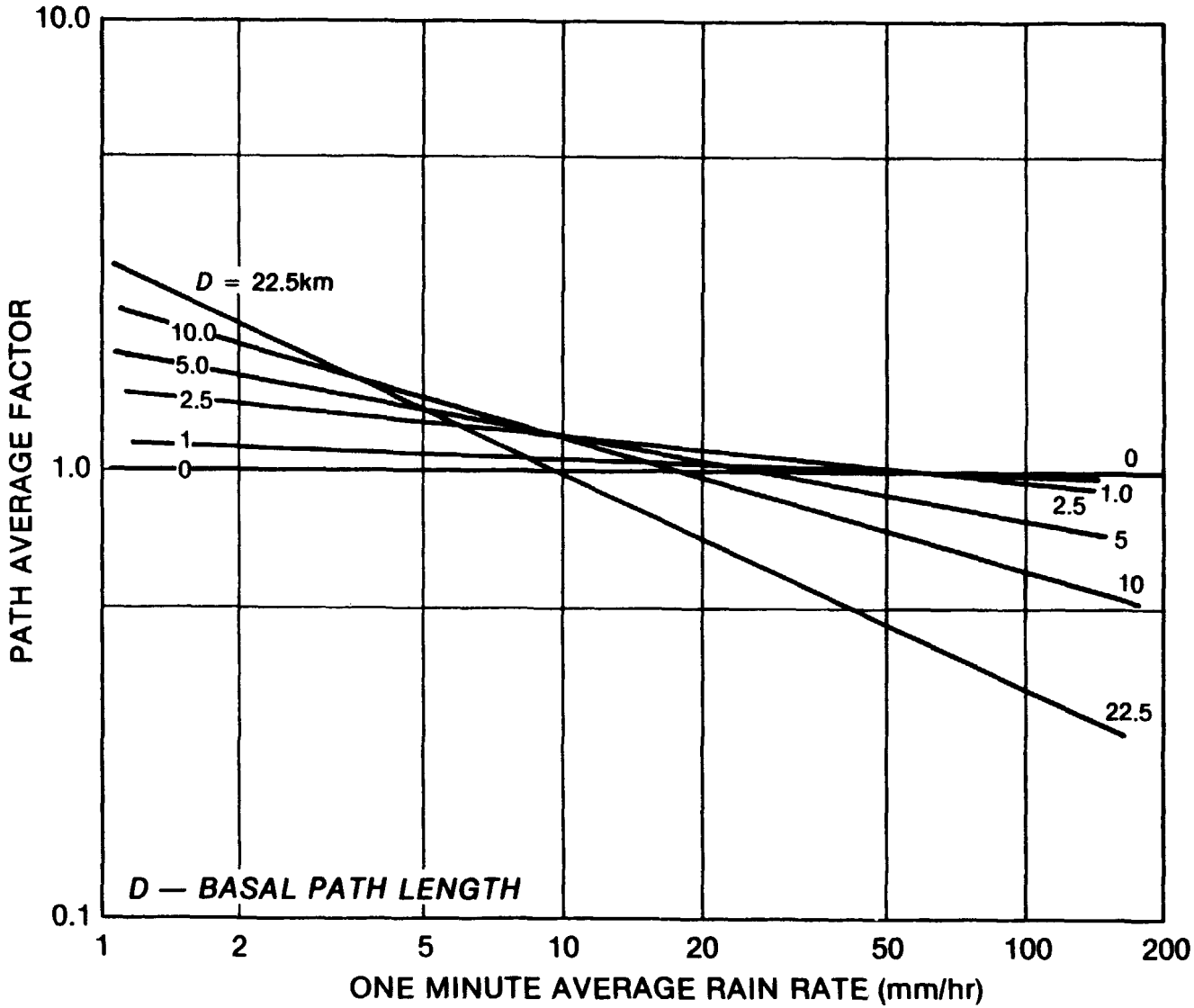

Figure 3.4-15. Effective Path Average Factor Model for Different Basal Path Lengths

where H is the height of the 0°C isotherm (see Figure 3.4-6b), θ is the elevation angle ($\theta > 10°$) and $D = H/\tan\theta$. For application at elevation angles lower than 10°, the effect of refraction by the troposphere and of the earth's curvature should be taken into account in the calculation of D. If D exceeds 22.5 km, a D_o of 22.5 km is used for the calculation of the effective path average factor and the occurrence probabilities are multiplied by D/D_o.

3.4.3.2 Variable Isotherm Height Technique. The variable isotherm height technique uses the fact that the effective height of the attenuating medium changes depending on the type of rainfall event. Also, various types of rainfall events selectively influence various percentages of time throughout the annual rainfall cycle. Therefore, a relation exists between the effective isotherm height and the percentage of time that the rain event occurs. This relation has been shown earlier in Figure 3.4-6a. Again the total attenuation is obtained by integrating the specific attenuation along the path. The resulting equation to be used for the estimation of slant path attenuation is:

$$A = \frac{a R_p^{\,b}}{\cos\theta}\left[\frac{e^{UZb}-1}{Ub} - \frac{X^b e^{YZb}}{Yb} + \frac{X^b e^{YDb}}{Yb}\right]; \theta \geq 10° \qquad (3.4\text{-}8)$$

where U, X, Y and Z are empirical constants that depend on the point rain rate. These constants are:

$$U = \frac{1}{Z}\left[\ln(Xe^{YZ})\right] \qquad (3.4\text{-}9)$$

$$X = 2.3\, R_p^{-0.17} \qquad (3.4.10)$$

$$Y = 0.026 - 0.03 \ln R_p \qquad (3.4\text{-}11)$$

$$Z = 3.8 - 0.6 \ln R_p \qquad (3.4\text{-}12)$$

for lower elevation angles $\theta < 10°$

$$A = \frac{L}{D}\, a\, R_p^{\,b} \left[\frac{e^{UZb}-1}{Ub} - \frac{X^b e^{YZb}}{Yb} + \frac{X^b e^{YDb}}{Yb} \right] \qquad (3.4\text{-}13)$$

where

$$L = [(E + H_g)^2 + (E + H_o)^2 - 2(E + H_g)(E + H_o)\cos\psi]^{1/2} \qquad (3.4\text{-}14)$$

$$= [(E + H_g)^2 \sin^2\theta + 2E(H_o - H_g) + H^2_0 - H^2_g]^{1/2} - (E + H_g)\sin\theta$$

ψ = path central angle defined above.

3-4.4 Application of the Global Model

Section 6.3.2.1 gives a step-by-step procedure for applying the Global Model, using the variable isotherm technique. Schwab (1980) applied this model on a worldwide basis to find downlink availability for specified margin and frequency. An example of the results of his work is shown in Figure 3.4-16. It is interesting to compare this figure with the rain climate region map of Figure 3.4-2.

3.5 THE TWO-COMPONENT MODEL

The Two-Component (T-C) rain attenuation model (Crane-1982) determines the probability of exceeding a given attenuation threshold. The Model's name relates to the fact that two distinctive types of rain events are addressed: convective cell and widespread "debris." The characterization of climatic zones is identical to the Global Model in terms of rain rates. The T-C Model was formulated in such a way that it might later be extended to site diversity systems, rain scatter interference, and attenuation duration statistics.

The fundamental approach in the T-C Model is to determine the probabilities for exceeding a given attenuation with convective rain and debris separately. The sum of these probabilities is then taken as the total probability of exceeding the given rain attenuation threshold.

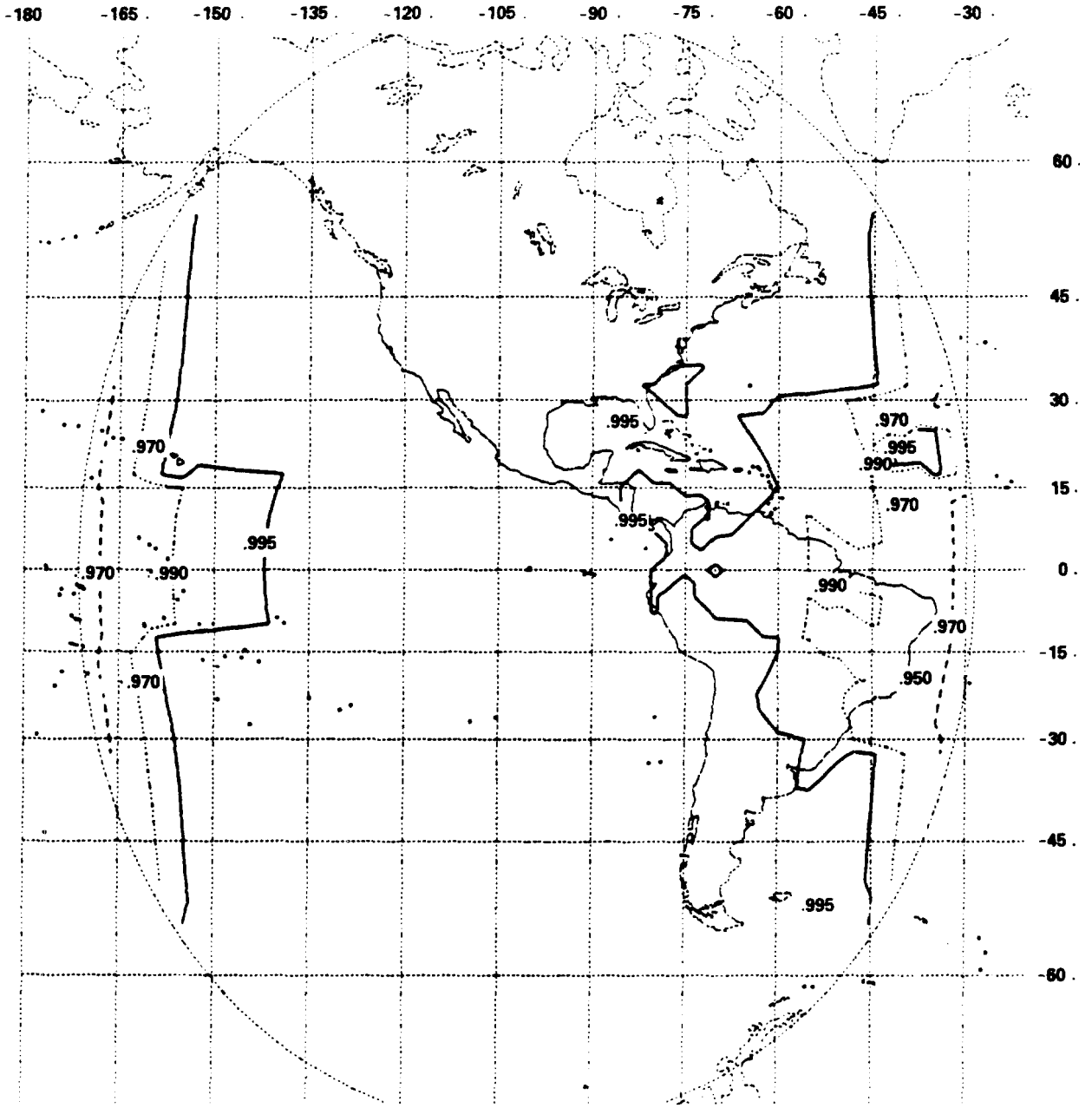

Figure 3.4-16. Availability Contours for Satellite at 100°W With 6 dB Margin Operating at 20 GHz

The projected (horizontal) path lengths for both types of rain are first determined geometrically from 0°C isotherm heights. These heights were modeled from observations during precipitation events using radiosonde data, rain occurrence data and excessive-precipitation data for seven spatially separated sites in the US (Crane-1980a). The data were extrapolated globally using averaged temperature profiles, where only summertime data was used at latitudes higher than 50°. The resulting height versus latitude variations, which do not employ the correlation between rain rate and rain rate height assumed in other models (e.g., Global), are:

$$H_c = 3.1 - 1.7 \sin [2(A-45)] \qquad (3.5\text{-}1)$$

$$H_d = 2.8 - 1.9 \sin [2(A-45)] \qquad (3.5\text{-}2)$$

where H_c, H_d are the rain heights in kilometers for volume cell (convective) and debris rain types, respectively, and A is the latitude (deg.). The corresponding projected path lengths are then determined geometrically as:

$$D_c D_d = \frac{(H_{c,d} - H_o)\,[2 - 2\,(H_{c,d} - H_o)/8500]}{\tan\theta \sqrt{\tan^2\theta + (H_{c,d} - H_o)/8500}} \qquad (3.5\text{-}3)$$

where Θ is the slant path elevation angle and H is height of the earth station above sea level (km).

The attenuation along the projected path is determined geometrically from the given slant path attenuation threshold and path elevation angle. This is then used to determine the corresponding rain rates, for volume cell and debris rain types, which would produce that amount of attenuation. The two rain types are addressed separately below.

3.5.1 Volume Cell Rain Rate

The average length of a line through a (circular) volume cell (W_c) is assumed to be about 2.2 km, based on the average volume cell

area data from a three year radar measurement program conducted in Goodland, Kansas. Thus, the effective projected path length through rain (L_c) must be taken to be the lesser of 2.2 km and D_c. If L_c is not determined from D_c ($D_c > W_c$), an adjustment factor (C) is required. In this case, the projected path D_c is longer than the average volume cell width and the integrated path rain rate must embody the effect of debris that is close to the cell. This is modeled as:

$$C = \frac{1 + 0.7\,(D_c - W_c)}{1 + (D_c - W_c)}\,;\ (D_c - 2.2) > 0 \qquad (3.5\text{-}4)$$

$$C = 1 \qquad ;(D_c - 2.2) \leq 0 \qquad (3.5\text{-}5)$$

The effective point rain rate (R') for volume cell rain can then be readily determined as:

$$R' = \left(\frac{CA}{KL_c}\right)^{1/\alpha} \qquad (3.5\text{-}6)$$

where A is the attenuation along the projected path and k and α are the common specific attenuation coefficients for point rainfall rates ($\gamma = KR^{\alpha}$).

3.5.2 Debris Rain Rate

In debris rain, the rain extent can readily exceed the slant path projection distance. The rain extent (W_d) is, however, dependent on rain rate. The Kansas radar observations indicated a relationship between average rain rate in debris and W_d:

$$W_d = 29.7R^{-0.34}$$